Investigation of Finite System-Size Effects in Molecular Dynamics Simulations of Lipid Bilayers

Francisco Castro-Román,[†,§] Ryan W. Benz,[‡] Stephen H. White,*[,†] and Douglas J. Tobias*[,‡]

Department of Physiology and Biophysics and Department of Chemistry, University of California, Irvine, California 92697-2025

Received: July 25, 2006; In Final Form: September 20, 2006

In the absence of external stress, the surface tension of a lipid membrane vanishes at equilibrium, and the membrane exhibits long wavelength undulations that can be described as elastic (as opposed to tension-dominated) deformations. These long wavelength fluctuations are generally suppressed in molecular dynamics simulations of membranes, which have typically been carried out on membrane patches with areas <100 nm^2 that are replicated by periodic boundary conditions. As a result, finite system-size effects in molecular dynamics simulations of lipid bilayers have been subject to much discussion in the membrane simulation community for several years, and it has been argued that it is necessary to simulate small membrane patches under tension to properly model the tension-free state of macroscopic membranes. Recent hardware and software advances have made it possible to simulate larger, all-atom systems allowing us to directly address the question of whether the relatively small size of current membrane simulations affects their physical characteristics compared to real macroscopic bilayer systems. In this work, system-size effects on the structure of a DOPC bilayer at 5.4 H_2O/lipid are investigated by performing molecular dynamics simulations at constant temperature and isotropic pressure (i.e., vanishing surface tension) of small and large single bilayer patches (72 and 288 lipids, respectively), as well as an explicitly multilamellar system consisting of a stack of five 72-lipid bilayers, all replicated in three dimensions by using periodic boundary conditions. The simulation results are compared to X-ray and neutron diffraction data by using a model-free, reciprocal space approach developed recently in our laboratories. Our analysis demonstrates that finite-size effects are negligible in simulations of DOPC bilayers at low hydration, and suggests that refinements are needed in the simulation force fields.

Introduction

In the past decade, molecular dynamics (MD) simulations have emerged as a powerful tool providing insights into the three-dimensional molecular structure and dynamics of lipid membranes that are not readily available from experimental methods. However, while simulation techniques continue to evolve, current empirical force fields used in typical biomolecular simulations are not without limitations or inaccuracies. For this reason, direct experimental measurements on membrane systems are critical to simulation techniques as they can provide important information needed to help refine force fields. In a recent simulation study of a DOPC bilayer at 66% relative humidity (RH),[1] it was found that current simulation force fields are not able to reproduce the experimental bilayer structure within experimental error. Understanding the source of these differences between the simulation and experimental data is crucial for advancing simulations of membrane systems.

One potential cause of the differences observed in the simulations may be artifacts due to the finite size of the simulated membrane systems. While the planar bilayer arrays and vesicles typically used in experiments are measured on the micrometer-scale, computational limitations allow, in practice, the simulation of only nanometer-scale membrane patches. The existence of finite-size effects in membrane simulations has been widely debated in the literature, and the discussion has mainly revolved around the proper ensemble in which to simulate small membrane patches.[2] Because unstressed bilayers adjust their area/molecule such that the free energy is minimized, and therefore have a surface tension $\gamma = 0$, it has been argued that the NPT (constant particle number, pressure, and temperature) ensemble should be employed in membrane simulations.[3,4] Others have suggested, however, that due to the small size of typical simulation membrane systems and the use of periodic boundary conditions, a nonzero surface tension may exist for small membrane patches at equilibrium due to the suppression of long wavelength undulations,[5] so that either a constant in-plane area ensemble (NPAT) or a constant surface tension ensemble (NPγT) is needed to accurately capture experimental membrane structure. To support this claim, Feller and Pastor reported the sensitivity of γ on the structural properties and size of simulated DPPC membranes.[5,6] However, Marrink and Mark found that the membrane area compressibility modulus depends on system size and in the stress-free regime ($\gamma = 0$), system size, has little effect on surface tension.[9] In another study, Lindahl and Edholm found that the area/lipid of simulated membranes can depend on system size when cutoff methods are used to calculate the electrostatic interactions.[7] However, when the particle-mesh Ewald summation (PME) method was used, only a slight dependence of system size on the area/lipid was found, with the area/lipid of a system consisting of 64 lipids differing less than 1 Å^2 from a system 16 times as large.[8]

* Address correspondence and reprint requests to these authors. E-mail: stephen.white@uci.edu (S.H.W.); dtobias@uci.edu (D.J.T.).

† Department of Physiology and Biophysics.

‡ Department of Chemistry.

§ Current address: Departamento de Física, Centro de Investigación y Estudios Avanzados del Instituto Politécnico National, A.P. 14-740, México Distrito Federal, Zacatenco CP 07360, Mexico.

10.1021/jp064746g CCC: $33.50
Published on Web 11/09/2006

Simulations performed in the NPAT and NPγT ensembles rely upon the availability of experimental data to provide an area/lipid at which to run the simulation. As the area/lipid of a fluid membrane is experimentally obtained through indirect measurements, and is sensitive to physical parameters such as hydration, lipid composition, and temperature, experimental area/lipid values are often not readily available. For NPAT and NPγT simulations that require this information, their use is limited, particularly for complex systems in which the area/lipid is both unknown and difficult to determine experimentally. To help address this problem, Klauda et al.[10] have suggested a method to determine the area/lipid computationally by running a series of simulations at different surface areas, and choosing the one that best fits the reciprocal-space diffraction data on that system. Though this method looks promising, additional studies on membranes of different lipid types beyond the DMPC membrane investigated will need to be considered, and the requirement to run possibly numerous simulations presents additional computational complexity.

Whether or not system size has an effect on simulation membrane structure, it is clear that both the membrane repeat distance, or *d*-spacing, and the area/lipid play a critical role in determining membrane structure. Indeed, membrane simulations performed at the correct surface area have yielded generally good membrane structures compared to experimental results.[10−12] In a systematic study of membrane simulation methodologies, Anézo et al.[12] found that accurate area/lipid values of simulated DPPC membranes could be obtained by using a variety of simulation protocols, and with such areas, other membrane structural quantities showed reasonable agreement with experimental data as well. However, when differences are observed between simulation and experimental *d*-spacing and area/lipid values, the underlying structure of the simulated bilayer will also show differences. Indeed, for the simulation study of a DOPC bilayer at 66% RH described above, significant differences were found between the experimental and simulation *d*-spacing and area/lipid values, contributing to the overall structural discrepancies observed.[1]

In addition to the differences in simulation *d*-spacing and area/lipid, significant differences were also found in the individual component-group distributions throughout the bilayer structure compared to the available X-ray and neturon diffraction data.[1] As these simulations were performed in the NPT ensemble, the main question we address here is whether these differences can be attributed to finite-size effects by comparing the structures of different sized membrane systems. If finite-size effects are found, this suggests that the NPAT or NPγT ensembles may in fact be required to simulate this system accurately. However, if finite-size effects are not present, the differences observed between the simulations and experimental results can be attributed to other sources, such as the force field. Furthermore, because undulations are not present in either the experimental or simulation results due to the low hydration used,[13,14] the issue of finite-size effects can be addressed for this system independent of undulation issues.

In the Methods section, a description of the investigated systems is presented along with a brief summary of the methods used to compare their structures. In the succeeding section, the real and reciprocal-space structures of the bilayer systems are compared with each other, as well as to experimental data, to assess the effect system size has on bilayer structure. Finally, in Discussion, the structural results are considered from which we conclude that finite-size effects contribute little to membrane structure for DOPC membranes at 66% RH, and suggest that the force field inaccuracies account for the large differences observed between the simulation and experimental data.

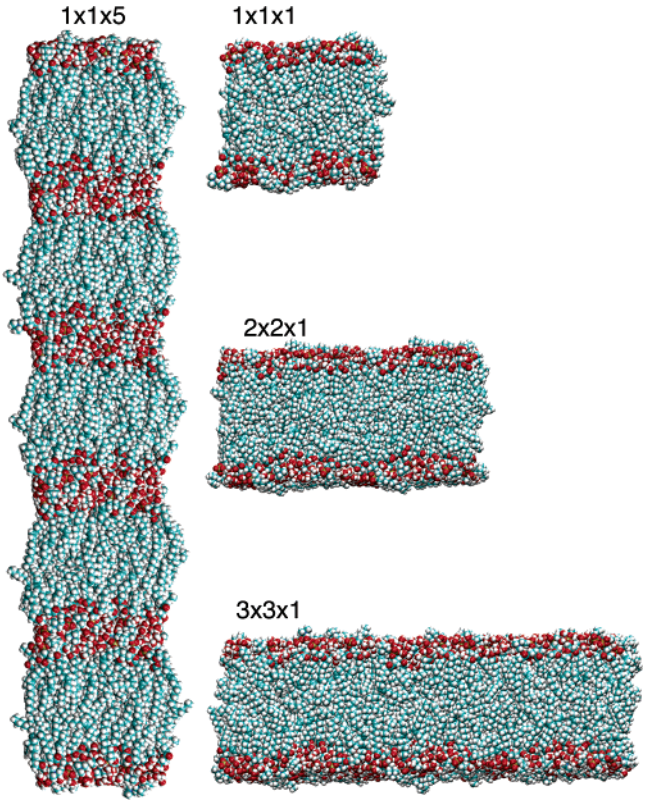

Figure 1. Images of the CHARMM27 membrane simulations. The initial system, consisting of 72 lipids (upper left corner), was replicated in the plane of the membrane to produce membrane patches 4 and 9 times larger than the original. A stack of 5 membranes (from the initial system) was also constructed, which represents the lamellar stacking found in experimental samples used for diffraction experiments.

Methods

Simulations. Simulations were performed with both the CHARMM27[11,15,16] and GROMOS lipid[17] force fields in the NPT ensemble at a temperature of 296 K and pressure of 1 atm. 3D periodic boundary conditions were used in all of the simulations. Prior to analysis of the trajectories, the center of mass was removed from each system at each frame. Specific details on the individual simulations are given below.

CHARMM27 Simulations. The NAMD molecular dynamics program, version 2.5,[18] was used with the CHARMM27 force field[11,15,16] to simulate several different-sized DOPC bilayer systems. The temperature was maintained by using Langevin dynamics with a collision frequency of 1 ps^{-1}. A fully flexible, orthorhombic cell was also used in conjunction with the Nosé−Hoover Langevin Piston algorithm[3,19] to maintain the system pressure. Electrostatic interactions were calculated by using the smooth particle-mesh Ewald (PME) summation method[20] with a grid spacing of ~1 Å, and the van der Waals interactions were switched smoothly to zero from 10 to 11 Å. The Verlet-I/r-RESPA method[21,22] was used to partition the simulation time steps as follows: 4 fs for the long-range electrostatic forces, 2 fs for the short ranged nonbonded forces, and 1 fs for the bonded forces. A neighbor list, updated every 8 steps, was also used with a radius of 12.5 Å.

The initial and smallest system consisted of 72 lipids and 386 waters giving a membrane hydration level of 66% RH or 5.4 waters/lipid, the same system extensively studied by Wiener

TABLE 1:

force field	system	no. of lipids	no. of waters	no. of atoms	simulation time (ns)	*d*-spacing (Å)	area/lipid (Å^2)
CHARMM27	1 × 1 × 1	72	386	11094	75	49.9 ± 0.57	57.3 ± 0.7
	2 × 2 × 1	288	1544	44376	10	50.4 ± 0.24	56.5 ± 0.27
	3 × 3 × 1	648	3474	99846	10	49.9 ± 0.17	57.3 ± 0.19
	1 × 1 × 5	360	1930	55470	20	50.4 ± 0.2	56.8 ± 0.7
GROMACS	2 × 2 × 1	288	1554	20214	10	49.7 ± 0.24	59.2 ± 0.31
	4 × 4 × 1	1152	6216	80856	7.7	49.7 ± 0.12	59.1 ± 0.15

and White.[14,23,24] The starting configuration was taken from the end of a previous simulation.[1] Two larger membrane patches were produced by replicating the original system in the membrane plane to give systems four and nine times larger. In the following text, the 72-lipid system will be referred to as 1 × 1 × 1, while the systems four and nine times larger will be referred to as 2 × 2 × 1 and 3 × 3 × 1, respectively. A fourth, multilamellar system was also constructed in which the 1 × 1 × 1 system was replicated in the transmembrane direction producing a stack of five, 72-lipid bilayers, referred to as 1 × 1 × 5. A summary of these systems is given in Table 1.

GROMACS Simulations. In addition to the CHARMM27 force field, simulations were also performed by using a modified GROMOS lipid force field,[17] with the GROMACS simulation package, version 3.1.4.[25] A fully flexible orthorhombic simulation cell was used with Berendsen pressure and temperature coupling.[26] The electrostatic interactions were calculated with the PME method[20] and a cutoff of 10 Å was used for the calculation of the Lennard-Jones interactions. A neighbor list, updated every 10 steps, was also used.

An initial system of 288 DOPC lipids and 1554 water molecules (2 × 2 × 1 using the naming convention here) was previously simulated and the ending configuration was used for the subsequent simulations. A system four times larger was also produced by replicating the initial system in the plane of the membrane, referred to as 4 × 4 × 1. The details on the composition of these systems are given in Table 1.

Structural Analysis. The structure factors and density profiles were determined by using the model-independent method described by Benz et al.[1] The intensity $I(s)$ scattered by a stack of membranes is related to the bilayer structure factor $F(s)$ and the interference function $G(s)$ by

$$I(s) = |F(s)\cdot G(s)|^2 \tag{1}$$

where s is the amplitude of the reciprocal space vector. $F(s)$ is the Fourier transform of the scattering X-ray or neutron density $\rho(z)$, which defines both the amplitude and phase of the scattered radiation by the atoms of the unit cell:

$$F(s) = \sum_{\text{unit cell}} f_i(s) e^{2\pi i s z} \tag{2}$$

where $f_i(s)$ represents the atomic form factor. The lattice function $G(s)$ consists of a series of delta functions spaced at intervals of d, the repeat distance, along the bilayer normal, i.e., the continuous Fourier transform $F(s)$ is only sampled at multiples of the Bragg condition h/d (h being the diffraction order). Assuming the bilayer profile is centrosymmetric, i.e., $\rho(z) = \rho(-z)$, the X-ray or neutron scattering-length density function can be determined via Fourier series reconstruction from the discrete structure factors $F(h)$ on the absolute scale by using

$$\rho(z) = \rho_0 + \frac{2}{d}\sum_{h=1}^{h_{max}} F(h)\cos\left(\frac{2\pi h z}{d}\right) \tag{3}$$

where h_{max} is the order of the highest observable order, d is the repeat lamellar distance, and $F(0)$ is the total scattering length in the unit cell

$$F(0)/d = \int_0^d \rho(z)\, dz = \rho_0 \tag{4}$$

Results

In-Plane CHARMM27 Systems. The simulated X-ray and neutron structure factors of the three CHARMM27 bilayer patches, determined from eq 2, are shown in Figure 2. The uncertainties for the simulated structure factors were determined by computing a set of structure factors, $\{F(h)\}$, at 1 ns intervals during the MD simulations and averaging over the resulting collection of configurations. Most of the simulated structure factors remain the same within error bars. Only a few diffraction

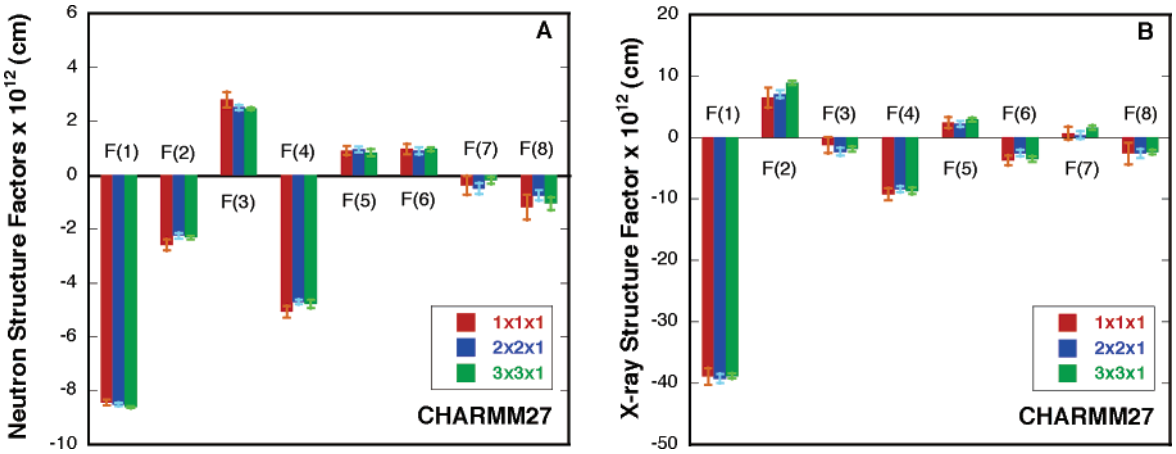

Figure 2. Neutron and X-ray structure factors for the CHARMM27 simulations. The neutron structure factors are shown in Panel A and the X-ray structure factors are shown in Panel B. The smallest system (1 × 1 × 1) is shown in red and the 2 × 2 × 1 and 3 × 3 × 1 systems are shown in blue and green, respectively. Eight orders of diffraction (structure factors) were computed for each of the CHARMM27 simulations. Only slight differences are seen among the values.

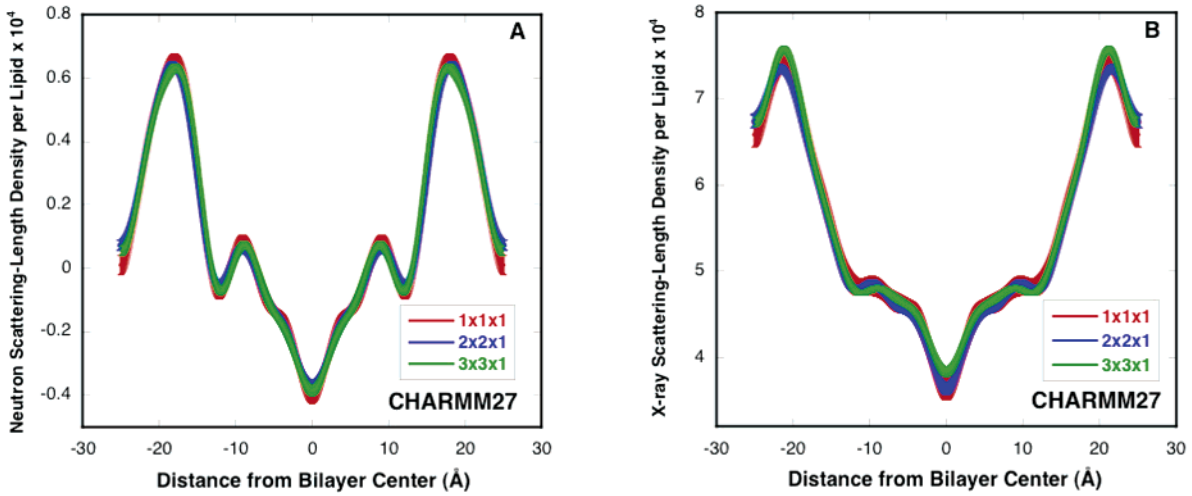

Figure 3. Neutron and X-ray scattering-length density profiles for the CHARMM27 simulations. By using the structure factors and associated error bars given in Figure 2, the corresponding scattering-length density profiles were calculated, with the neutron and X-ray results shown in Panels A and B, respectively. The $1 \times 1 \times 1$ results are shown in red, the $2 \times 2 \times 1$ results are shown in blue, and the $3 \times 3 \times 1$ results are shown in green. In the profiles, the thickness of the curves corresponds to the uncertainty in density at each position in space. As with the structure factors, virtually no differences are observed among the systems, within experimental error.

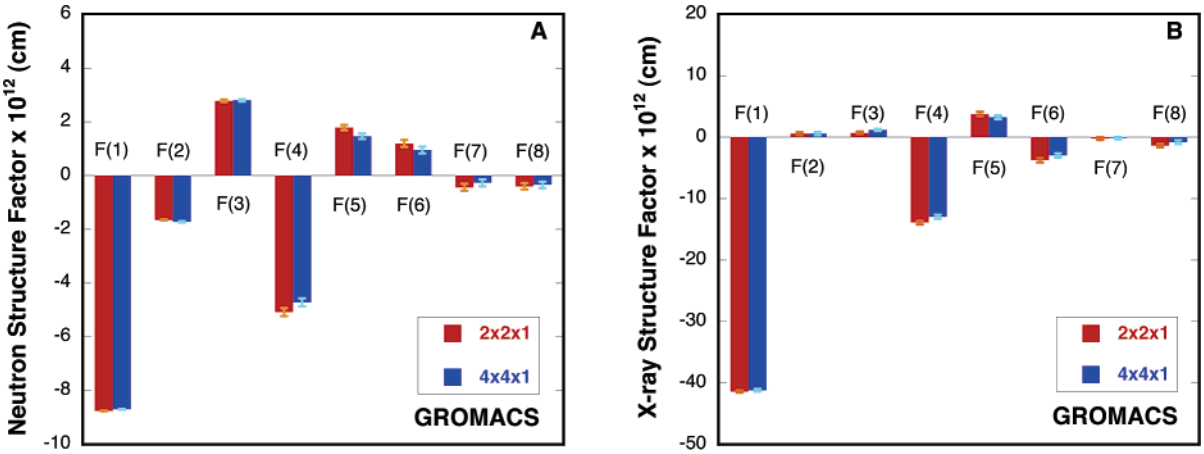

Figure 4. Neutron and X-ray structure factors for the GROMACS simulations. The $2 \times 2 \times 1$ and $4 \times 4 \times 1$ results are shown in red and blue, respectively, with the neutron results given in Panel A and the X-ray results given in Panel B. The eight orders of diffraction are shown for the two simulated GROMACS simulations. The error bars show that both sets of data are essentially the same within experimental error.

orders show slight differences between the different bilayer patches at the edges of the error bars: the 2nd and 4th orders for the X-ray data, and the 5th order for the neutron data. Overall, however, these differences have little effect on the real space density profiles.

The structure factors shown in the bar charts of Figure 2 were used to compute density profiles by means of eq 3. The associated uncertainties of the structure factors and the Box−Muller algorithm[27] were used to generate a set of mock structure factors, from which confidence bands of the profiles (see ref 1) were produced, indicated by the thickness of the curves. The simulated CHARMM27 structure of the three patches remains essentially the same, as shown by the almost perfect superposition of the X-ray and neutron scattering-length density profiles within the indicated error bands in Figure 3. The slight mismatch in the X-ray scattering length trough and headgroup heights between the $3 \times 3 \times 1$ and the smaller patches is due to the bigger mean scattering density $\rho_0 = F(0)/d$ caused by a smaller repeat-distance in the $3 \times 3 \times 1$ system ($d = 49.9$ Å) compared to 50.4 and 50.5 Å for the $2 \times 2 \times 1$ and $1 \times 1 \times 1$ systems, respectively. This repeat distance effect on the scattering-length density profiles is more pronounced in the case of X-rays (see eq 4) as the X-ray total scattering length is always much bigger than the total neutron scattering length, which in general is close to zero for lipid bilayers. A summary of the average *d*-spacing and area/lipid values for the different membrane systems is presented for comparison in Table 1.

GROMACS Systems. As in the analysis of the CHARMM27 data, the GROMACS configurations were sampled every nanosecond to determine the real and reciprocal-space structures of the $2 \times 2 \times 1$ and $4 \times 4 \times 1$ systems. As the lipid hydrogens are treated implicitly in the GROMOS force field, the X-ray and neutron scattering lengths of the CH, CH_2, and CH_3 groups were treated as the sum of carbon and hydrogen scattering lengths reflecting their united atom nature. The average structure factors are essentially the same in both X-ray and neutron reciprocal space for the two bilayer patches, as shown in Figure 4. Minute differences can be seen in the 3rd and 4th X-ray orders and the 4th neutron order. However, these differences translate into negligible changes on the real-space density profiles.

The X-ray and neutron density profiles for the $2 \times 2 \times 1$ and $4 \times 4 \times 1$ bilayer patches, calculated via Fourier reconstruction of the structure factors shown in Figure 4, are presented in Figure 5. The scattering-length density profiles practically overlap within error bars for both the X-ray and neutron data. The slight differences observed in the CHARMM27

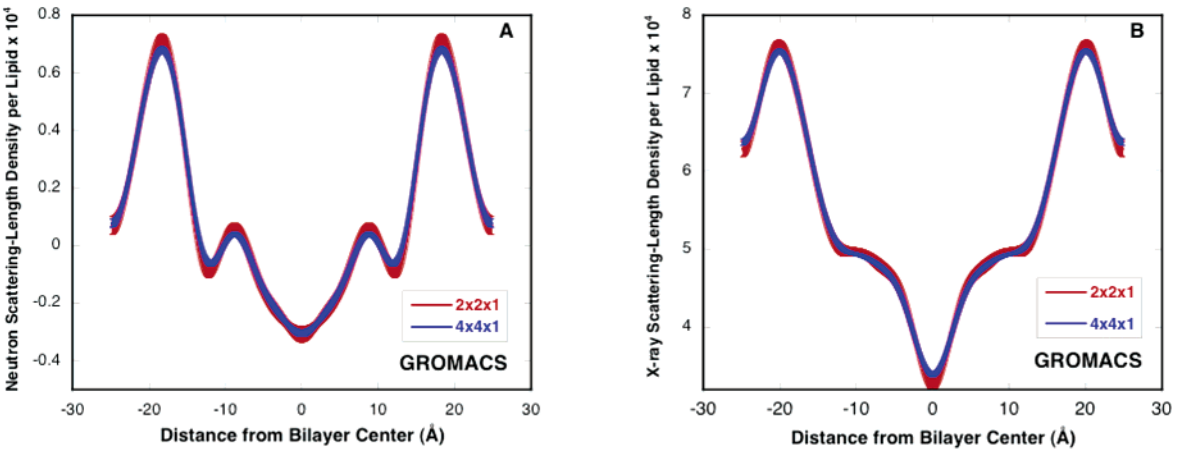

Figure 5. Neutron and X-ray scattering-length density profiles for GROMACS simulations. Panel A shows the neutron profiles and Panel B shows the X-ray profiles. The 2 × 2 × 1 profiles are shown in red and the 4 × 4 × 1 profiles are shown in blue. Like the previous results, no differences are seen among the GROMACS density profiles.

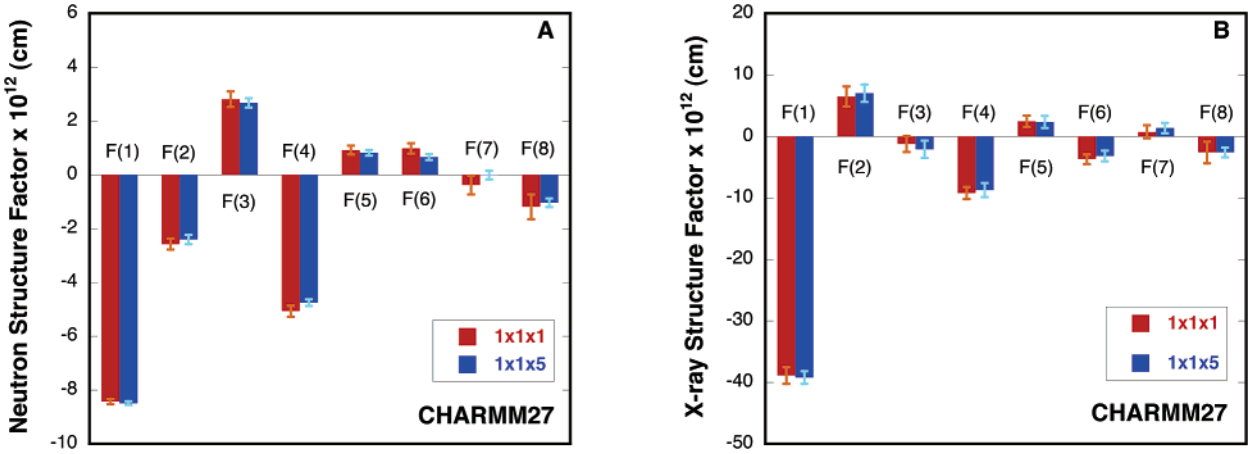

Figure 6. Neutron and X-ray structure factors for the CHARMM27 membrane stack (blue) and the 1 × 1 × 1 system (red). The neutron and X-ray results are shown in Panels A and B, respectively. Unlike the previous systems, the system considered here consists of a stack of membranes (see Figure 1). However, despite the differences in the physical representation of the system, the structure factors are virtually the same as those of the smallest system, 1 × 1 × 1.

X-ray density profiles due to the repeat-distance difference are not present in the GROMACS data because in this case the cell dimensions remain virtually unchanged. The average *d*-spacing and area/lipid values for the GROMACS systems are shown in Table 1.

Multilamellar CHARMM27 System. As explained in the Methods section, the structure factors for the single bilayer patches were obtained by sampling the continuous Fourier transform at intervals of *h*/*d*. This is possible because the single bilayer or unit cell is replicated an infinite number of times in the *z* direction with use of periodic boundary conditions. Hence, the interference function can be described as a series of delta functions. For a unit cell consisting of a stack of bilayers, eq 2 does not produce a continuous function. Instead, it directly gives the diffraction pattern of the simulated stack. Figure 6 shows the neutron and X-ray structure factors of an explicitly multilamellar system consisting of a stack of five 72-lipid bilayers compared to the corresponding 1 × 1 × 1 system structure factors. All of the X-ray and neutron structure factors agree within error bars and the scattering densities perfectly overlap (Figure 7), showing no significant size effects on the structure of the lipid bilayer.

Comparison to Experimental Data. The CHARMM27 and GROMACS X-ray and neutron scattering-length density profiles of the largest systems simulated are compared to the corresponding experimental[14] profiles in Figure 8. As was previously observed for the 2 × 2 × 1 system,[1] none of the simulated profiles agree with the experimentally determined profiles within experimental error. With both force fields, generally good agreement between the simulation and experimental results is found in the membrane interior (±10 Å from the bilayer center), with the exception of the GROMACS neutron profile. As neutron diffraction is sensitive to hydrogens, the differences in this region can be attributed, in part, to the GROMACS united atom representation of the carbon chains, in which the hydrogens are not explicitly represented. Away from the membrane interior, significant differences are found between simulation and experimental scattering-length density profiles, particularly around the interfacial region. For the CHARMM27 simulations, the main headgroup peaks are shifted away from the bilayer center, apparent in both the X-ray and neutron profiles. A similar trend is observed in the GROMACS neutron profile, though the X-ray scattering-length density shows relatively good agreement throughout the profile, consistent with the accurate *d*-spacing and area/lipid for this system.

To further understand the simulation membrane structures, we compare in Figure 9 the component-group distribution parameters corresponding to the 1 × 1 × 1 and 3 × 3 × 1 CHARMM27 systems with the experimental values determined by a joint refinement method combining X-ray and neutron

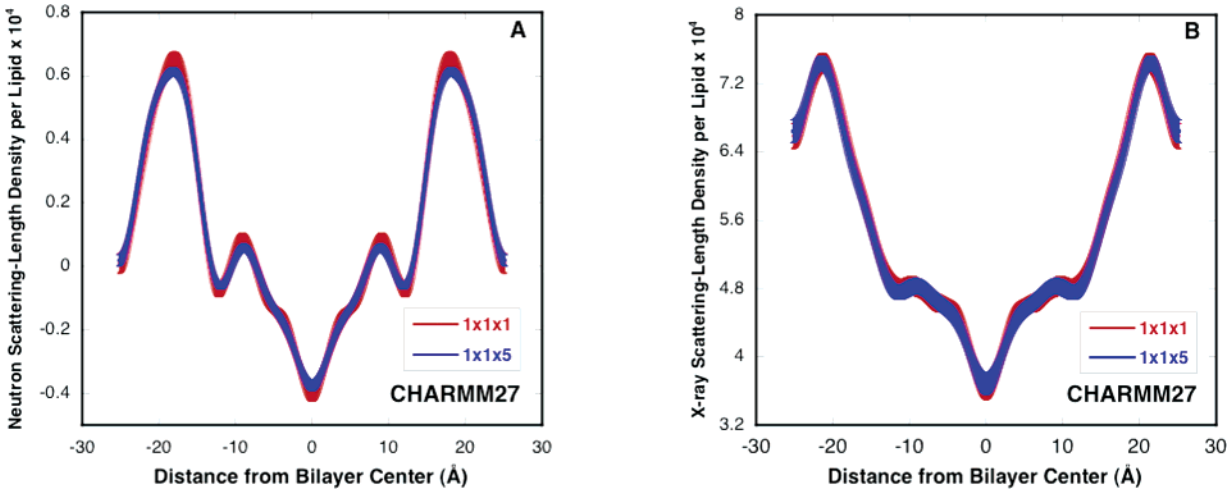

Figure 7. Neutron and X-ray scattering-length density profile for the membrane stack. Both the $1 \times 1 \times 1$ planar membrane system (red) and the stack of membranes (blue) give the same neutron (Panel A) and X-ray (Panel B) structures within experimental error.

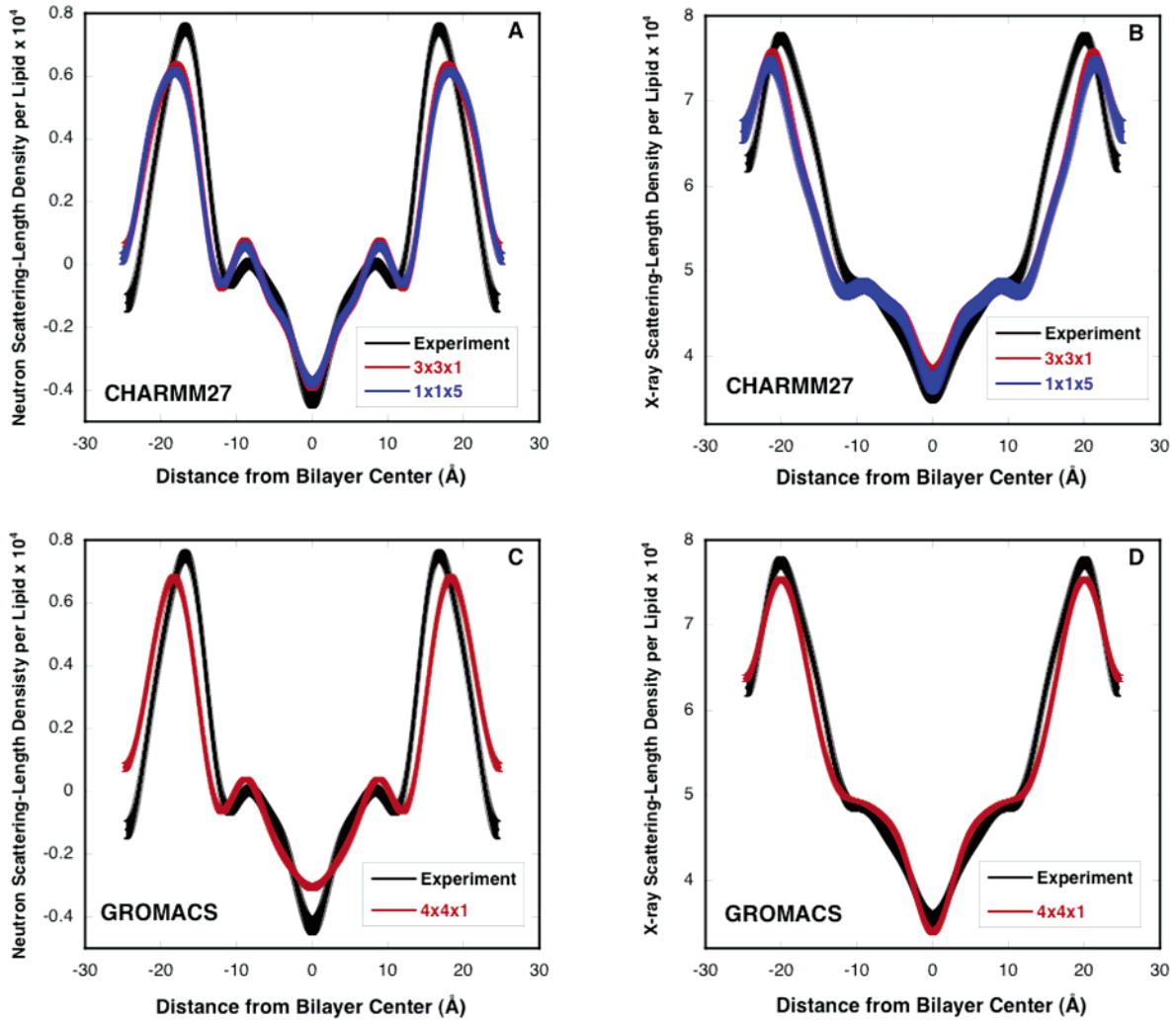

Figure 8. Comparison of the simulated and experimental scattering-length density profiles. Though the simulations (red and blue), regardless of system size, give the same bilayer structure, discrepancies still exist compared to the experimental profiles[14] (black). Because finite-size effects have been shown not to be the source of the inconsistencies, force field refinement may be necessary.

diffraction data.[14] Because the component-group distribution parameters provide information about how the membrane molecular components (such as the phosphate, double bond, and water groups) are distributed in the system, they can provide a more detailed view of membrane structure compared to the scattering-length density profiles. Consistent with the results above, the $1 \times 1 \times 1$ and $3 \times 3 \times 1$ systems show very similar distribution parameters, indicating that the internal membrane structures are essentially the same. However, a comparison of the simulation and experimental results shows significant

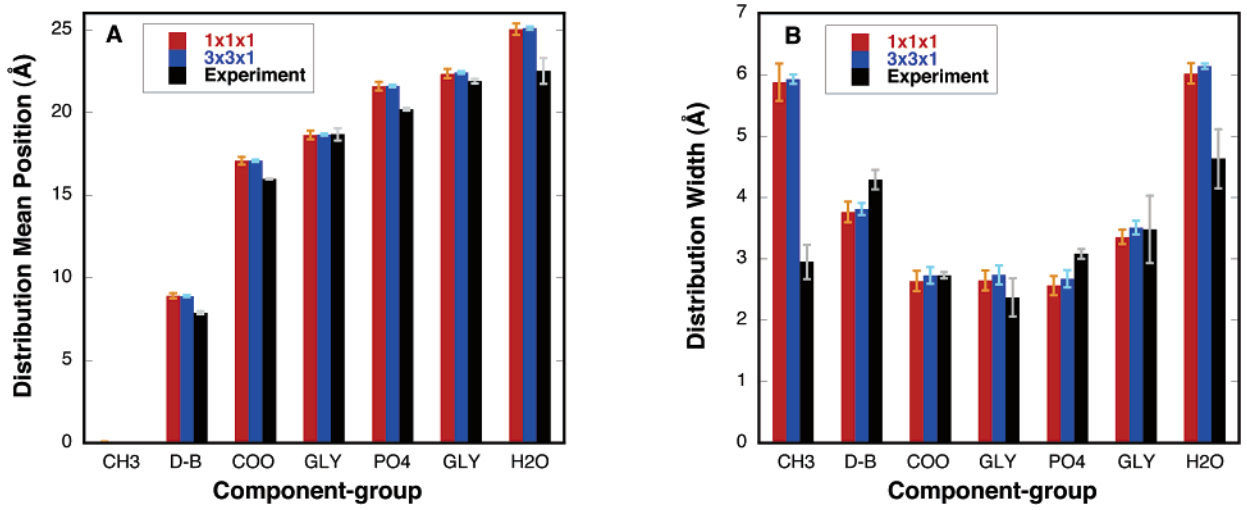

Figure 9. Comparison of the simulated and experimentally determined mean positions and widths of the molecular component groups in DOPC and water for the CHARMM27. (A) The simulated mean positions show no change as the bilayer patch size is increased by a 9 to 1 ratio. (B) Very small differences are observed on the molecular component widths of the $1 \times 1 \times 1$ and $3 \times 3 \times 1$ systems. These differences all fall within the error bars of the measurements, however, indicating no finite-size effects. The persistence of the differences between experimental[14] and simulated distributions means and widths at different system sizes suggests that discrepancies with the experimental values might reside in the force field itself.

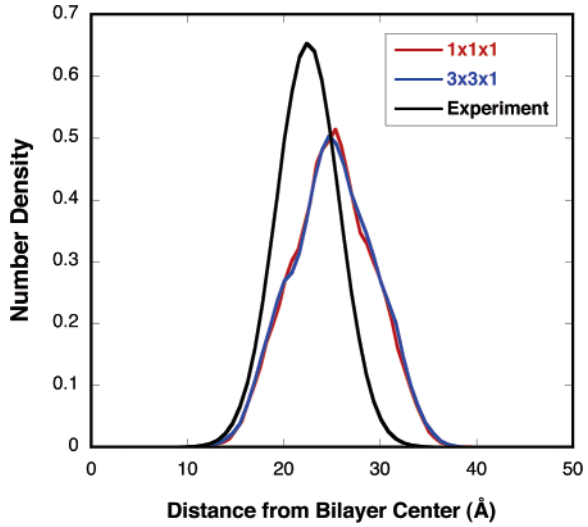

Figure 10. Comparison of simulation and experimental water distributions. Though nine times larger, the $3 \times 3 \times 1$ system (blue) has essentially the same water distribution as the $1 \times 1 \times 1$ system (red). Compared to the experimental distribution (black), however, the simulation results show significant differences. In particular, the simulation distribution means are shifted away from the bilayer center and the distribution widths are larger. These differences suggest inaccurate hydration of the membrane lipids in the simulations.

differences in both the distribution means and widths for the majority of the component-group distributions, consistent with previous results.[1]

In the interfacial region of the membrane systems, the simulation water-component distribution parameters show particularly strong differences compared to the experimental parameters. The actual water distributions for the CHARMM27 $1 \times 1 \times 1$ and $3 \times 3 \times 1$ systems, compared to the experimental distribution, are given in Figure 10. Consistent with the previous observations that system size has little effect on the membrane structure, both simulations give essentially the same water distribution. Compared to the experimental distribution, the simulations show a shifting of the distribution mean away from the bilayer center and a widening of the distribution width.

Discussion

As discussed in the Introduction, simulations of lipid bilayers using the CHARMM force fields have typically been performed in the NPAT ensemble, motivated by the idea that the small bilayer patches used in MD simulations suppress long wavelength undulations, and therefore require an applied surface tension to make up for the suppression.[5] As a result, discrepancies in simulated bilayer structure, when simulated in the NPT ensemble, compared to experiment have been attributed to finite-size effects. Indeed, simulations performed in the NPAT ensemble with use of the experimental area/lipid typically give much better structural results compared to NPT simulations, which generally underestimate the area/lipid and overestimate the *d*-spacing. When the correct membrane surface area is achieved in simulations, other structural properties tend to show good agreement with experimental data as well.[12] Another potential and likely source for structural errors may be due to force field inaccuracies, which can be masked when constant area/surface tension constraints are used in membrane simulations.

By using the structural results from simulations of several different-sized bilayer systems using two different force fields, the issue of finite-size effects for DOPC bilayers at 66% RH can be directly addressed. On the basis of the recent comparison of simulated and experimental membrane structure,[1] as well as the results shown here, it is clear that finite-size effects do not significantly contribute to the observed structural discrepancies between the simulation and experimental results. While significant differences are observed between the simulation and experimental scattering-length density profiles (Figures 8 and 9), virtually no structural differences are seen between the various simulation systems investigated here (Figures 2−7). Though this study only considers DOPC bilayers at low hydration, the fact that structural differences still exist between the simulation and experimental data for this system, which cannot be attributed to finite-size effects to any significant degree, suggests that further refinement to the CHARMM lipid parameters is necessary. Analysis of the simulation profiles obtained here can give insight into where refinement is needed.

The comparison of the scattering-length density profiles in Figure 8 shows relatively good agreement between simulation and experimental profiles in the middle region of the bilayer. However, toward the interfacial region, the simulation and experimental profiles diverge, suggesting that lipid headgroup, water, and/or their interaction parameters need refinement. The comparison of the component-group distribution parameters in Figure 9 also supports this conclusion. In particular, the large differences in the water simulation distribution means and widths compared to the experimental values for the water group indicate that proper hydration of the lipid headgroups is not being achieved in the simulations. The actual water distributions presented in Figure 10 show that the waters are essentially being pushed out of the membrane interface compared to the experimental distribution, which is more localized in the headgroup region. As membrane area/lipid has been shown to depend strongly on hydration, particularly for DOPC bilayers,[28,29] properly capturing membrane hydration is critical for accurate membrane force fields.

The ultimate goal of molecular simulations is to replace the need to perform physical experiments with in silico calculations. While there is still much work to do to advance scientific computational methods, small steps can be taken by recognizing the current inaccuracies and limitations of the empirical force field. Through critical investigation of simulation methodologies along with subsequent refinement, this can help to advance not only the understanding of our computational models, but also the systems that they are based upon.

Acknowledgment. This research was supported in part by NSF Grant CHE-0417158 to D.J.T., NIH grants GM68002, RR14812, and GM46823 to S.H.W., and National Research Service Award 5 T15 LM00744 from the National Library of Medicine to R.W.B. NAMD was developed by the Theoretical and Computational Biophysics Group at the Beckman Institute for Advanced Science and Technology at the University of Illinois at Urbana−Champaign.

References and Notes

(1) Benz, R. W.; Castro-Román, F.; Tobias, D. J.; White, S. H. *Biophys. J.* **2005**, *88*, 805.

(2) Scott, H. L. *Curr. Opin. Struct. Biol.* **2002**, *12*, 495.

(3) Tu, K.; Tobias, D. J.; Klein, M. L. *Biophys. J.* **1995**, *69*, 2558.

(4) Jähnig, F. *Biophys. J.* **1996**, *71*, 1348.

(5) Feller, S. E.; Pastor, R. W. *Biophys. J.* **1996**, *71*, 1350.

(6) Feller, S. E.; Pastor, R. W. *J. Chem. Phys.* **1999**, *111*, 1281.

(7) Lindahl, E.; Edholm, O. *Biophys. J.* **2000**, *79*, 426.

(8) Wohlert, J.; Edholm, O. *Biophys. J.* **2004**, *87*, 2433.

(9) Marrink, S. J.; Mark, A. E. *J. Phys. Chem. B* **2001**, *105*, 6122.

(10) Klauda, J. B.; Kucerka, N.; Brooks, B. R.; Pastor, R. W.; Nagle, J. F. *Biophys. J.* **2006**, *90*, 2796.

(11) Feller, S. E.; Yin, D. X.; Pastor, R. W.; MacKerell, A. D., Jr. *Biophys. J.* **1997**, *73*, 2269.

(12) Anézo, C.; de Vries, A. H.; Höltje, H.-D.; Tieleman, D. P.; Marrink, S.-J. *J. Phys. Chem. B* **2003**, *107*, 9424.

(13) Smith, G. S.; Safinya, C. R.; Roux, D.; Clark, N. A. *Mol. Cryst. Liq. Cryst.* **1987**, *144*, 235.

(14) Wiener, M. C.; White, S. H. *Biophys. J.* **1992**, *61*, 434.

(15) Schlenkrich, M.; Brickmann, J.; MacKerell, A. D., Jr.; Karplus, M. An empirical potential energy function for phospholipids: Criteria for parameter optimization and applications. In *Biological Membranes*; Merz, K. M., Jr., Roux, B., Eds.; Birkhäuser: Boston, MA, 1996; p 31.

(16) Feller, S. E.; MacKerell, A. D., Jr. *J. Phys. Chem. B* **2000**, *104*, 7510.

(17) Berger, O.; Edholm, O.; Jähnig, F. *Biophys. J.* **1997**, *72*, 2002.

(18) Kalé, L.; Skeel, R.; Bhandarkar, M.; Brunner, R.; Gursoy, A.; Krawetz, N.; Phillips, J.; Shinozaki, A.; Varadarajan, K.; Schulten, K. *J. Comput. Phys.* **1999**, *151*, 283.

(19) Feller, S. E.; Zhang, Y.; Pastor, R. W.; Brooks, B. R. *J. Chem. Phys.* **1995**, *103*, 4613.

(20) Essmann, U.; Perera, L.; Berkowitz, M. L.; Darden, T.; Lee, H.; Pedersen, L. G. *J. Chem. Phys.* **1995**, *103*, 8577.

(21) Grubmüller, H.; Heller, H.; Windemuth, A.; Schulten, K. *Mol. Simul.* **1991**, *6*, 121.

(22) Tuckerman, M.; Berne, B. J. *J. Chem. Phys.* **1992**, *97*, 1990.

(23) Wiener, M. C.; King, G. I.; White, S. H. *Biophys. J.* **1991**, *60*, 568.

(24) Wiener, M. C.; White, S. H. *Biophys. J.* **1992**, *61*, 428.

(25) Berendsen, H. J. C.; van der Spoel, D.; van Drunen, R. *Comput. Phys. Commun.* **1995**, *91*, 43.

(26) Berendsen, H. J. C.; Postma, J. P. M.; van Gunsteren, W. F.; DiNola, A.; Haak, J. R. *J. Chem. Phys.* **1984**, *81*, 3684.

(27) Press, W. H.; Flannery, B. P.; Teukolsky, S. A.; Vetterling, W. T. *Numerical Recipes. The Art of Scientific Computing*; Cambridge University Press: Cambridge, UK, 1989.

(28) Tristram-Nagle, S.; Petrache, H. I.; Nagle, J. F. *Biophys. J.* **1998**, *75*, 917.

(29) Hristova, K.; White, S. H. *Biophys. J.* **1998**, *74*, 2419.